Physics of Fluids

Erratum: "A constitutive hemorheological model addressing both the deformability and aggregation of red blood cells" [Phys. Fluids 32, 103103 (2020)]

Cite as: Phys. Fluids **33**, 039901 (2021); https://doi.org/10.1063/5.0043721
Submitted: 11 January 2021 . Accepted: 19 February 2021 . Published Online: 18 March 2021

Pavlos S. Stephanou

Physics of Fluids ERRATUM scitation.org/journal/phf

Erratum: "A constitutive hemorheological model addressing both the deformability and aggregation of red blood cells" [Phys. Fluids 32, 103103 (2020)]

Cite as: Phys. Fluids **33**, 039901 (2021); doi: 10.1063/5.0043721
Submitted: 11 January 2021 · Accepted: 19 February 2021 ·
Published Online: 18 March 2021

View Online Export Citation CrossMark

Pavlos S. Stephanou[a)]

AFFILIATIONS

Department of Chemical Engineering, Cyprus University of Technology, P.O. Box 50329, 3603 Limassol, Cyprus

[a)]Author to whom correspondence should be addressed: pavlos.stefanou@cut.ac.cy. Tel.: +357-25-002394. Fax: +357-25-002668.

https://doi.org/10.1063/5.0043721

The sentence in Sec. II A of Stephanou[1] "Considering the typical values $2a = 7.5\,\mu$m and $V_{RBC} = 90\,\mu$m^3, we must consider $c = 3.06\,\mu$m." should be replaced by "If we, then, consider the typical values $2a = 7.5\,\mu$m and $V_{RBC} = 90\,\mu$m^3, we must consider $2c = 3.06\,\mu$m."

Also, the sentence "In the following, we make the choice $\mathbf{g} = -\lambda\mathbf{C}$ that duly satisfies the requirement that the Poisson bracket fulfills the Jacobi identity" just after Eq. (10) in Sec. II C should be replaced by "In the following, we make the choice $\mathbf{g} = -2\lambda(\mathbf{S}/\mathrm{tr}\mathbf{S}) = -2\lambda(\mathbf{B}/\mathrm{tr}\mathbf{B})$, which duly satisfies the requirement that the Poisson bracket fulfills the Jacobi identity." This change, which also slightly modifies the predictions as we will illustrate below, stems from the fact that the choice $\mathbf{g} = -\lambda\mathbf{C}$ is *not* thermodynamically admissible, whereas $\mathbf{g} = -2\lambda(\mathbf{S}/\mathrm{tr}\mathbf{S})$ is. In more detail, as illustrated by Öttinger,[2] when $\mathbf{g} = g_1\mathbf{B} + g_2\boldsymbol{I} + g_3\mathbf{B}^{-1}$ with, in general, $g_k = g_k(\lambda, I_1, I_2, I_3)$, $k = \{1, 2, 3\}$, where $I_1 = \mathrm{tr}\mathbf{B}$, $I_2 = \mathrm{ln}\mathrm{det}\mathbf{B}$, and $I_3 = -\mathrm{tr}\mathbf{B}^{-1}$ are the three invariants of the dimensionless unconstrained conformation tensor $\mathbf{B}$, then the following constrains should hold:

$$\begin{aligned} g_1\frac{\partial g_2}{\partial\lambda} - g_2\frac{\partial g_1}{\partial\lambda} &= 2\left(\frac{\partial g_1}{\partial I_2} - \frac{\partial g_2}{\partial I_1}\right),\\ g_1\frac{\partial g_3}{\partial\lambda} - g_3\frac{\partial g_1}{\partial\lambda} &= 2\left(\frac{\partial g_1}{\partial I_3} - \frac{\partial g_3}{\partial I_1}\right),\\ g_2\frac{\partial g_3}{\partial\lambda} - g_3\frac{\partial g_2}{\partial\lambda} &= 2\left(\frac{\partial g_2}{\partial I_3} - \frac{\partial g_3}{\partial I_1}\right). \end{aligned} \tag{E1}$$

Since $\mathbf{S} = \mathbf{B}/(\mathrm{det}\mathbf{B})^{1/3}$ and $\mathbf{C} = \mathbf{S}\cdot\mathbf{S}_{eq}^{-1}$, the expression originally considered $\mathbf{g} = -\lambda\mathbf{C}$ means that $g_1 = g_1(\lambda, I_3)$ and $g_2 = g_3 = 0$, which, however, is forbidden by Eq. (E1). On the other hand, the new expression $\mathbf{g} = -2\lambda(\mathbf{S}/\mathrm{tr}\mathbf{S}) = -2\lambda(\mathbf{B}/\mathrm{tr}\mathbf{B})$ means that $g_1 = g_1(\lambda, I_1)$ and $g_2 = g_3 = 0$, which is permitted by Eq. (E1).

Equation (15a) should be

$$\begin{aligned} \dot{S}_{\alpha\beta,[JS]} &= -\frac{3(1-\lambda)}{I_2^C\tau_S}\left[-\left(S_{\alpha\gamma}S^{-1}_{eq,\gamma\zeta}S_{\zeta\beta} - \frac{I_1^C}{3}S_{\alpha\beta}\right)\right.\\ &\quad\left. -\frac{2I_2^C}{3}\left(S_{eq,\alpha\beta} - \frac{I_2^C}{3}S_{\alpha\beta}\right)\right],\\ \frac{D\lambda}{Dt} &= -\frac{1}{\tau_\lambda}\mathrm{ln}\lambda - \frac{2\lambda}{\mathrm{tr}\mathbf{S}}(\nabla\mathbf{u})^T : \mathbf{S}. \end{aligned} \tag{15a}$$

Equation (16) should be

$$\begin{aligned} \sigma_{\alpha\beta} &= \frac{6\eta_s}{\tau_s}Htf_0(1-\xi)\left(I_1^C S_{\alpha\gamma}S^{-1}_{eq,\gamma\beta} - S_{\alpha\gamma}S^{-1}_{eq,\gamma\eta}S_{\eta\zeta}S^{-1}_{eq,\zeta\beta} - \frac{2I_2^C}{3}\delta_{\alpha\beta}\right)\\ &\quad -\frac{6\eta_s}{\tau_s}Htf_0\frac{\lambda\mathrm{ln}\lambda}{\mathrm{tr}\mathbf{S}}S_{\alpha\beta} + \eta_\infty(Ht,\lambda_\eta)\dot{\gamma}_{\alpha\beta}. \end{aligned} \tag{16}$$

Equation (17) should be

$$\begin{aligned} \tilde{\sigma}_{\alpha\beta} &= 6Htf_0(1-\xi)\left(I_1^C S_{\alpha\gamma}S^{-1}_{eq,\gamma\beta} - S_{\alpha\gamma}S^{-1}_{eq,\gamma\eta}S_{\eta\zeta}S^{-1}_{eq,\zeta\beta} - \frac{2I_2^C}{3}\delta_{\alpha\beta}\right)\\ &\quad -6Htf_0\frac{\lambda\mathrm{ln}\lambda}{\mathrm{tr}\mathbf{S}}S_{\alpha\beta} + P(Ht,\lambda_\eta)\tilde{\gamma}_{\alpha\beta}. \end{aligned} \tag{17}$$

Due to this correction regarding the expression for $\mathbf{g}$, some predictions presented in Figs. 2–8 of Stephanou[1] are in error. The corrected figures are shown in Figs. 2–8 below. The new choice of $\mathbf{g}$ induces a lesser dependence of the ε parameter on the shear stress and shear viscosity predictions (Figs. 2 and 3). Furthermore, the new choice of $\mathbf{g}$ leads to similar predictions for N_1 and $-N_2$ as illustrated in Figs. 4 and 5.

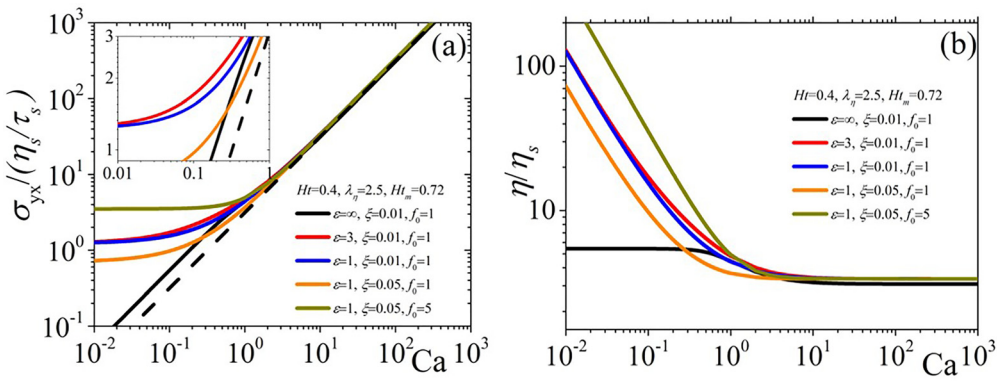

FIG. 2. Model predictions for the dimensionless (a) shear stress and (b) shear viscosity as a function of Ca for various values of the parameters ξ, f_0, and ε while keeping $\lambda_\eta = 2.5$, $Ht = 0.4$, and $Ht_m = 0.72$ fixed. The dotted line in panel (a) depicts the Newtonian contribution of $P(Ht, \lambda_\eta)$Ca.

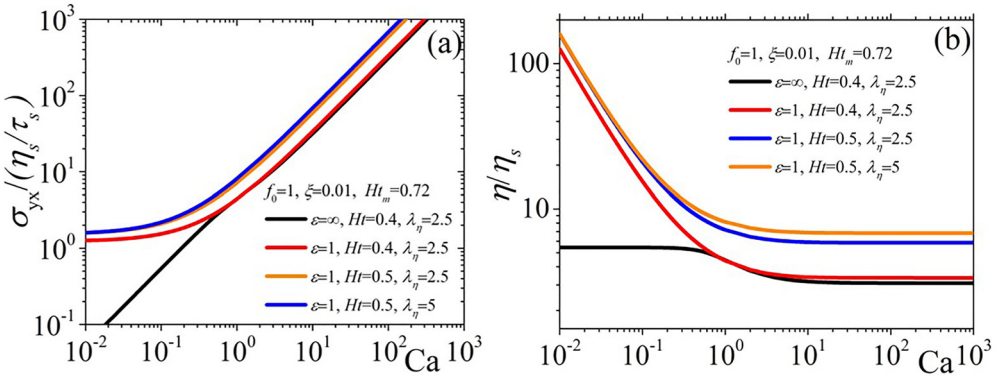

FIG. 3. Model predictions for the dimensionless (a) shear stress and (b) shear viscosity as a function of Ca for various values of the parameters ε, Ht, and λ_η while keeping $\xi = 0.01$, $f_0 = 1$, and $Ht_m = 0.72$ fixed.

In particular, the parameter ε is now seen to induce similar changes in the predictions of both N_1 and $-N_2$. Also, by increasing the parameter ξ the effect on $-N_2$ is not a simple shift upwards.

Note that the value of some parameters has been modified. Specifically, in Fig. 2 the value of $\xi = 0.05$ instead of $\xi = 0.1$ was employed to provide the predictions depicted in orange and dark yellow, respectively; in Figs. 4 and 5, the value of $\xi = 0.05$ instead of $\xi = 0.1$ was employed to provide the prediction depicted in orange; and in Fig. 6, the value of $\xi = 0.02$ instead of $\xi = 0.05$ was employed to provide the prediction depicted in orange.

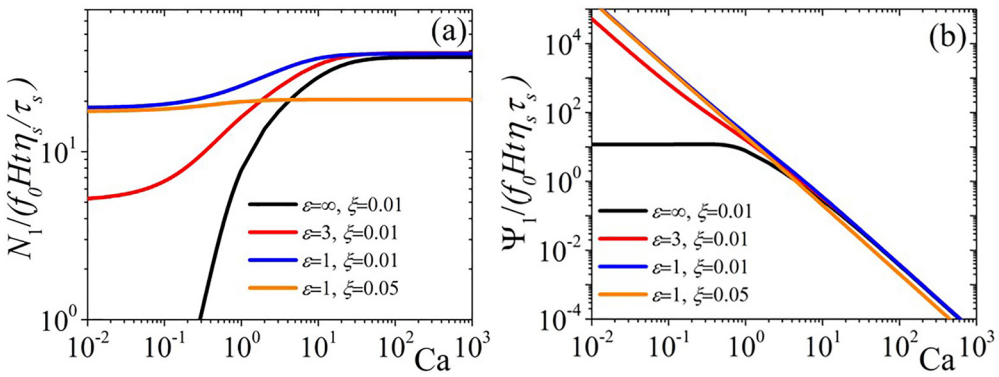

FIG. 4. Model predictions for the dimensionless (a) first normal stress difference and (b) first normal stress coefficient as a function of Ca for various values of the model parameters ξ and ε.

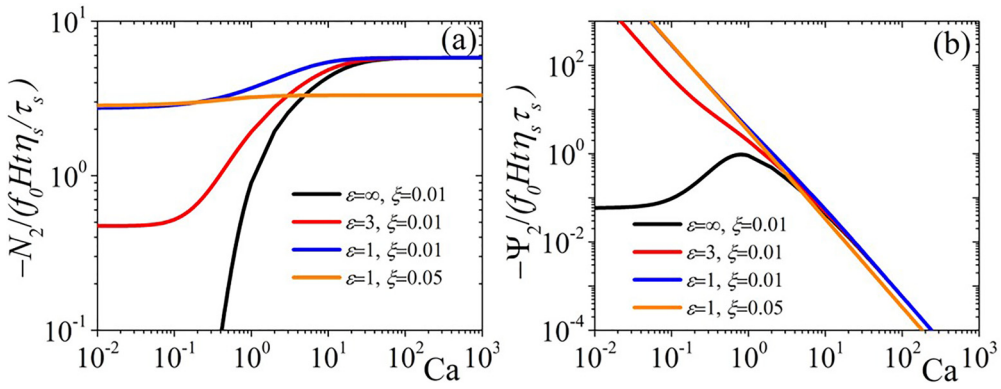

FIG. 5. Model predictions for the negative dimensionless (a) second normal stress difference and (b) second normal stress coefficient as a function of Ca for various values of the model parameters ξ and ε.

The comparison with experimental data is depicted in Figs. 7 and 8. Note that in Fig. 8, the value of $f_0 = 4.5$ instead of $f_0 = 4.2$ was employed. We believe that it is important to stress the significance of each of the model parameters and clarify which can be considered as adjustable parameters. Overall, there are four parameters (the slip/nonaffine parameter ξ, the ratio between the two relaxation times, $\varepsilon = \tau_\lambda/\tau_S$, which controls the appearance of a yield point, the parameter f_0, and the characteristic relaxation time related to the deformability of a RBC, τ_S) that are freely adjusted to fit experimental data and three more (the hematocrit Ht, the ratio between the internal and external viscosities, λ_η, and the solvent viscosity, η_S) that should be available from the experimental setup. The slip/nonaffine parameter, in particular, controls the form of the Johnson–Segalman (JS) time derivative given in Eq. (15b) of Stephanou:[1] when interested in incompressible and homogeneous flows, for $\xi = 0$, the JS time derivative reduces to the upper-convected Maxwell time derivative, for $\xi = 1$ to

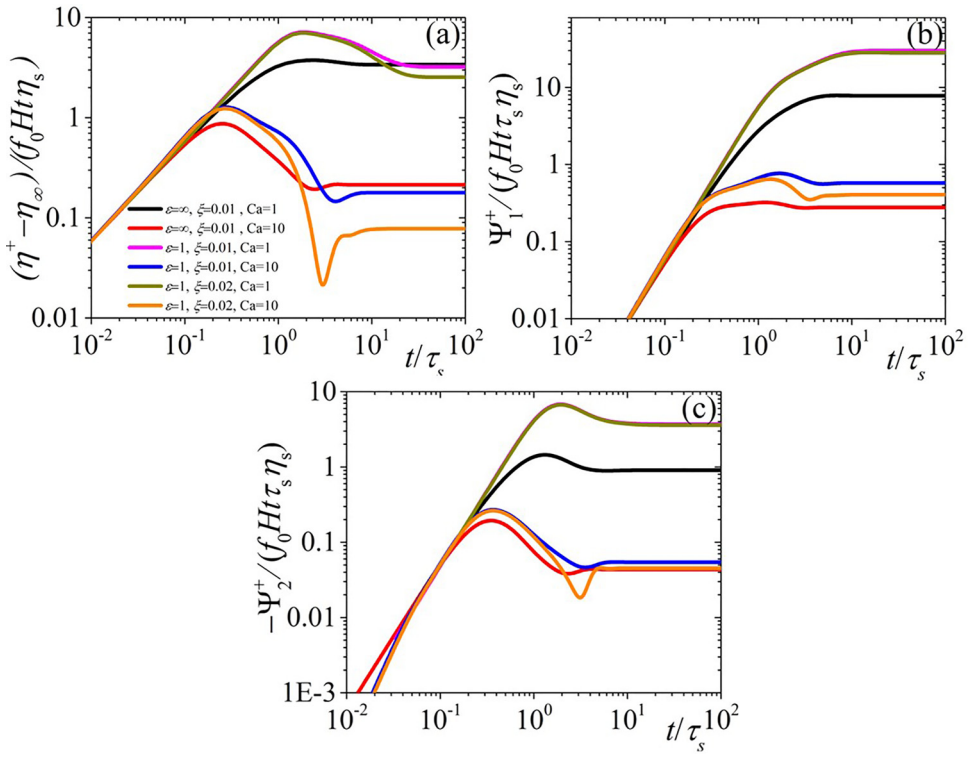

FIG. 6. Growth of the dimensionless (a) shear viscosity, (b) first normal stress coefficient, and (c) second normal stress coefficient upon the inception of simple shear flow at different Ca for various values of the parameters ξ and ε.

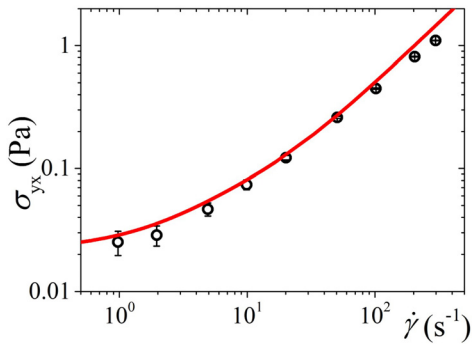

FIG. 7. Comparison of the model predictions (red line) for the shear stress with the experimental rheological data at $T = 37\,^{\circ}$C (circles) of the blood of donor A from Sousa *et al.*[3] with $Ht = 0.416$. Here, $Ht_m = 0.72$, $\eta_S = 1.2$ mPa s, $\lambda_\eta = 5$, $\xi = 0.01$, $\varepsilon = 5$, $f_0 = 1$, and $\tau_S = 0.06$ s.

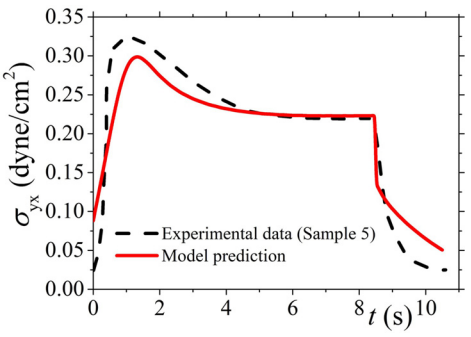

FIG. 8. Comparison of the model predictions (continuous red line) with the experimental step-change in shear rate data (dashed black line) of normal blood sample 5 of Bureau *et al.*[4] at $T = 25\,^{\circ}$C. Here, Ht=0.45, $Ht_m = 0.72$, $\eta_S = 1.8$ mPa s, $\lambda_\eta = 5$, $\xi = 0.01$, $\varepsilon = 30$, $f_0 = 4.5$, and $\tau_S = 1$ s.

the corotational time derivative, whereas for $\xi = 2$ to the lower-convected Maxwell time derivative. In the extreme case $\xi = 1$, upon inception of flow the RBCs would immediately start tumbling without deforming, meaning that the elastic contribution to the stress vanishes. For $\xi > 0$, tumbling occurs after some critical shear rate is reached, which also results in the appearance of a dumping behavior, i.e., the appearance of an undershoot following the overshoot, in the transient material functions at sufficiently large shear rates (see Fig. 6), as also noted in the case of the transient shear viscosity of polymer solutions (see Stephanou *et al.*[5]) The normal blood data reported by Sousa *et al.*[3] state that the hematocrit of the sample prepared is $Ht = 41.6\%$, whereas Bureau *et al.*[4] do not report it; for this reason, when comparing against the experimental data of Bureau *et al.*[4] we assume a physiological value of $Ht = 45\%$. Also, we consider the average value of $\lambda_\eta = 5$, whereas the value of the plasma viscosity η_S is taken from literature values. The value of ξ is chosen small enough to avoid spurious oscillations in the transient behavior of both $\boldsymbol{S}$ and the material functions. When comparing model predictions with the experimental data, we simply consider $\xi = 0.01$. The remaining three parameters $(\varepsilon, f_0, \tau_S)$ are selected to best fit the experimental data.

As a final comment, we should point out that RBCs do not only tumble but a wealth of dynamical states have been noted experimentally, such as tank-treading and rolling;[6] in addition, simulation[7,8] and experimental studies[9] in single cell dynamics have shown that the transition between these dynamical states depends on the viscosity ratio, λ_η: when $\lambda_\eta = 1$ a tumbling to tank-treading behavior is expected as the shear rate increases, while when $\lambda_\eta = 5$ more severe shape changes are expected. Recent smoothed dissipative particle dynamics simulations[7] have also indicated that tumbling is hindered in concentrated suspensions. These conclusions point to the fact that the slip parameter should actually be a function of other parameters, such as the hematocrit and the viscosity ratio.

Finally, the sentence at the end of Sec. IV of Stephanou[1] "considering $\varepsilon = 30$, $f_0 = 4.2$," should be replaced by "considering $\varepsilon = 30$, $f_0 = 4.5$."

REFERENCES

[1]P. S. Stephanou, "A constitutive hemorheological model addressing both the deformability and aggregation of red blood cells," Phys. Fluids **32**, 103103 (2020).
[2]H. C. Öttinger, *Beyond Equilibrium Thermodynamics* (John Wiley and Sons, 2005).
[3]P. C. Sousa, J. Carneiro, R. Vaz, A. Cerejo, F. T. Pinho, M. A. Alves, and M. S. N. Oliveira, "Shear viscosity and nonlinear behavior of whole blood under large amplitude oscillatory shear," Biorheology **50**, 269 (2013).
[4]M. Bureau, J. C. Healy, D. Bourgoin, and M. Joly, "Etude rhéologique en régime transitoire de quelques échantillons de sangs humains artificiellement modifiés," Rheol. Acta **18**, 756 (1979).
[5]P. S. Stephanou, T. Schweizer, and M. Kröger, "Communication: Appearance of undershoots in start-up shear: Experimental findings captured by tumbling-snake dynamics," J. Chem. Phys. **146**, 161101 (2017).
[6]J. Dupire, M. Socol, and A. Viallat, "Full dynamics of a red blood cell in shear flow," Proc. Natl. Acad. Sci. U. S. A. **109**, 20808–20813 (2012).
[7]W. Chien, G. Gompper, and D. A. Fedosov, "Effect of cytosol viscosity on the flow behavior of red blood cell suspensions in microvessels," Microcirculation **28**, e12668 (2021).
[8]A. Z. K. Yazdani and P. Bagchi, "Phase diagram and breathing dynamics of a single red blood cell and a biconcave capsule in dilute shear flow," Phys. Rev. E **84**, 026314 (2011).
[9]T. M. Fischer and R. Korzeniewski, "Threshold shear stress for the transition between tumbling and tank-treading of red blood cells in shear flow: Dependence on the viscosity of the suspending medium," J. Fluid Mech. **736**, 351 (2013).